



Applying a support vector model to assess land cover changes in the Uvs Lake Basin ecoregion in Mongolia

Buyan-Erdene Jamsran^a, Chinsu Lin^{a,*}, Ishgaldan Byambakhuu^b, Jamsran Raash^c, Khaulenbek Akhmadi^d

^a Department of Forestry and Natural Resources, National Chiayi University, 300 University Rd., Chiayi, Chiayi 60004, Taiwan, China

^b Department of Environment and Forest Engineering, School of Engineering and Applied Sciences, National University of Mongolia, Mongolia

^c Uvs Lake Basin Projected Area Administration Office, Uvs Province, Mongolia

^d Head of Division for Desertification Study, Institute of Geography and Geoecology, Mongolian Academy of Sciences, Mongolia

ARTICLE INFO

Article history:

Received 10 May 2018

Received in revised form

24 June 2018

Accepted 29 July 2018

Available online 2 August 2018

Keywords:

Land suppression

Soil degradation

Forest reduction

Change analysis

Landscape ecology

ABSTRACT

The Uvs Lake Basin in western Mongolia is a natural world heritage site and is known for its diversity in landscape and wildlife. Recently, investigative research has shown that the protected pristine ecotone is suffering land degradation due to global warming. In order to obtain evidence of the changes over a long-term time scale, serial multi-temporal Landsat images obtained between 1995 and 2015 were used to classify land cover and land cover changes over the Basin ecoregion using a machine learning classification technique, support vector machine. Results showed that the forest land area in 1995 was 1888.48 km² which was equivalent to 7.48% of the total area of the study site. The forest area showed considerable decrease by 301.36 km² during the first decade (1995–2004) and 155.81 km² during second decade (2004–2015). A total of 457.17 km² or 24.21% of the forest land has been developed, most being changed into grassland. The major driver of such changes was illegal logging, forest fire, and pest damage. However grassland was changed primarily into bare land during the two decades. The area of glacier was decreased and primarily changed into water body. In contrast, the area of sand in the Basin ecoregion increased dramatically from 65.20 km² in 1995 to 318.33 km² in 2015 the increase being mostly from the transition of bare land. In summary, the drivers of the significant decrease of greenness coverage and increase of sand/bare land areas were the interaction of complicated disturbances in both anthropogenic and natural factors, in which logging, grazing, wind erosion, and global warming were the key causes.

© 2018 China Agricultural University. Production and hosting by Elsevier B.V. on behalf of KeAi. This is an open access article under the CC BY-NC-ND license (<http://creativecommons.org/licenses/by-nc-nd/4.0/>).

1. Introduction

Land cover changes affect atmospheric, climatic and biological spheres of the Earth [1,2]. The physical characteristics of the surface, seen in the distribution of forest, vegetation,

* Corresponding author.

E-mail address: chinsu@mail.ncyu.edu.tw (C. Lin).

Peer review under responsibility of China Agricultural University.

<https://doi.org/10.1016/j.inpa.2018.07.007>

2214-3173 © 2018 China Agricultural University. Production and hosting by Elsevier B.V. on behalf of KeAi.

This is an open access article under the CC BY-NC-ND license (<http://creativecommons.org/licenses/by-nc-nd/4.0/>).

water, soil and other physical attributes of the land that are due to the influence of human habitation, with an emphasis on the functional role of land for economic activities, have been drawing the attention of the worldwide political and scientific community [3].

The Great Lakes Basin in Mongolia consists of the Great Lakes and the surrounding lands of the provinces of Uvs, Khovd, Bayan-Olgii, Zavkhan, and Govi-Altai. The Uvs Lake Basin and the Hyargas Lake Basin located in the area of Uvs Province are the two major Basins in Mongolia. The Uvs Lake Basin ecoregion consisting of the Uvs Nuur Lake, wetland, sand dunes and marshes sitting beside the mountain and forests was listed as a natural World Heritage Site by UNESCO in 2003 due to the natural steppe landscapes which provide habitats for endangered wildlife, waterfowl mitigation, biodiversity, and also contain valuable historical archeological and cultural features. The Great Lakes Basin contains the most important wetlands of Central Asia, situated at this ecotone region in western Mongolia [4] where meteorological data and ground inspection have shown that global warming has been affecting land degradation over the protected basin [2,5]. Such degradation will in turn further impact pasture degradation, surface and groundwater resources [2].

The Uvs Lake Basin was recognized as a nationally protected natural landscape in 1993 [5] and the landscape of the site can be seen as a forest-grassland-desert ecotone with a steep geographical change. This area is ecosystems shaped by the extreme climate and still scarcely influenced by human factors such as overgrazing, soil erosion, salinization, degradation and increasing human activities [6]. Therefore, this area was selected as part of the International Geosphere and Biosphere Programme (IGBP), one of 10 sites over the world for global climate change study [7]. Information about the specific site with regards to changes of land cover would be of great interest.

Remotely sensed data provided a diversity of spectral and canopy height information which is valuable for exploring biophysical and biochemical properties of forests [3], carbon stocks and productivity of terrestrial ecosystems [8–10], parameters of individual trees [11–14] and forest stand [15], mapping of land use and land cover [1,16]. One of the most important benefits of the satellite for observing the earth is the monitoring of land development or changes [17] supplying quantitative analysis of the spatial distribution of the population of interest [18]. Recently, much research [2,19–23] has tried to examine the changes of land cover in Mongolia using a variety of resources satellite images such as SPOT, Landsat, and MODIS. An interesting result of studies using MODIS EVI images for the assessment of pasture vegetative coverage was the observation that the pasture biomass significantly decreased from 33% to 66% during the period from 2001 to 2011 in the Uvs Province [5]. According to the land resources census carried out in 2011, some 17.7% or 838.3 km² of pastureland out of the total basin area was degraded by overgrazing [5]. Obviously, the changes of grassland biomass have become a problem for sustainable ecosystem management of the protected Uvs Lake Basin [6,23]. Beyond the grassland, changes of other land covers of the terrestrial ecosystem such as forest, dessert steppe, and desert can provide additional

evidence of climate change and/or the degradation over such sub-ecosystems.

As mentioned, a few researchers have explored the changes of land covers [20,22] and net primary production of the Mongolian terrestrial ecosystems [21] using moderate resolution (pixel size in hundred meter) of satellite images. However, in this case a rare attempt was made to examine the land cover changes of the particular area of Uvs Lake Basin (hereafter the Basin). In order to obtain evidence of changes over a relative small area to address natural and anthropogenic impacts on the protected area, a series of land cover classification needed to be made using satellite images with spatial resolution better than 250/500-meter resolution MODIS images, for example the Landsat images with 30-meter pixels.

The approach of exploring land cover change can be quantitative or qualitative. A quantitative method detects the change of spectral information of a pixel vector via a normalized data such as atmospherically corrected reflectance image. This requires post processing to define what the meaning of a change vector is. In contrast, a qualitative method involves two particular steps: land cover classification and change analysis. This firstly defines land cover map for each of multi-temporal images and then draws the change path of land cover for each pixel. In contrast to the former method, the later one is an easier way to derive change paths of the land cover and is therefore a direct and spatially explicit method for retrieving information of land cover transition [1].

Support vector machine (SVM) is a non-parametric machine learning algorithm which is theoretically able to catch crucial spectral signatures via only a few training sample (support vectors) deriving the hyperplane to achieve reliable and satisfied land cover classification [1]. The hyperplane generated via the SVM training process is very consistent over a variety of field observations including accounting for the prominent role of elevation, slope, humidity and micro-topography on plant distribution [24]. Many studies [1,13,25–31] have shown the ability of SVM in land cover mapping and suggest it would be an appropriate method for deriving the changes of land cover using 30-meter resolution Landsat images. Therefore, the objective of this study was to explore the changes of land cover in the Uvs Lake Basin ecoregion over latest two decades using multi-temporal Landsat multispectral images. This work also extended to comparison of the appropriateness of the classifiers SVM and MLC as the later has been generally applied to map land cover distribution in Mongolia for years.

2. Material and methods

2.1. Study area

Fig. 1 shows the location of the Uvs Lake Basin in western Mongolia with a small part in Russia (white parts within the red box of sub-Fig. 1B). The climate condition in the Uvs Lake Basin is strongly continental and semi-arid, characterized by long cold winters, dry, windy springs, relatively hot summers (30 °C), and a short growing season of 158 days from April to

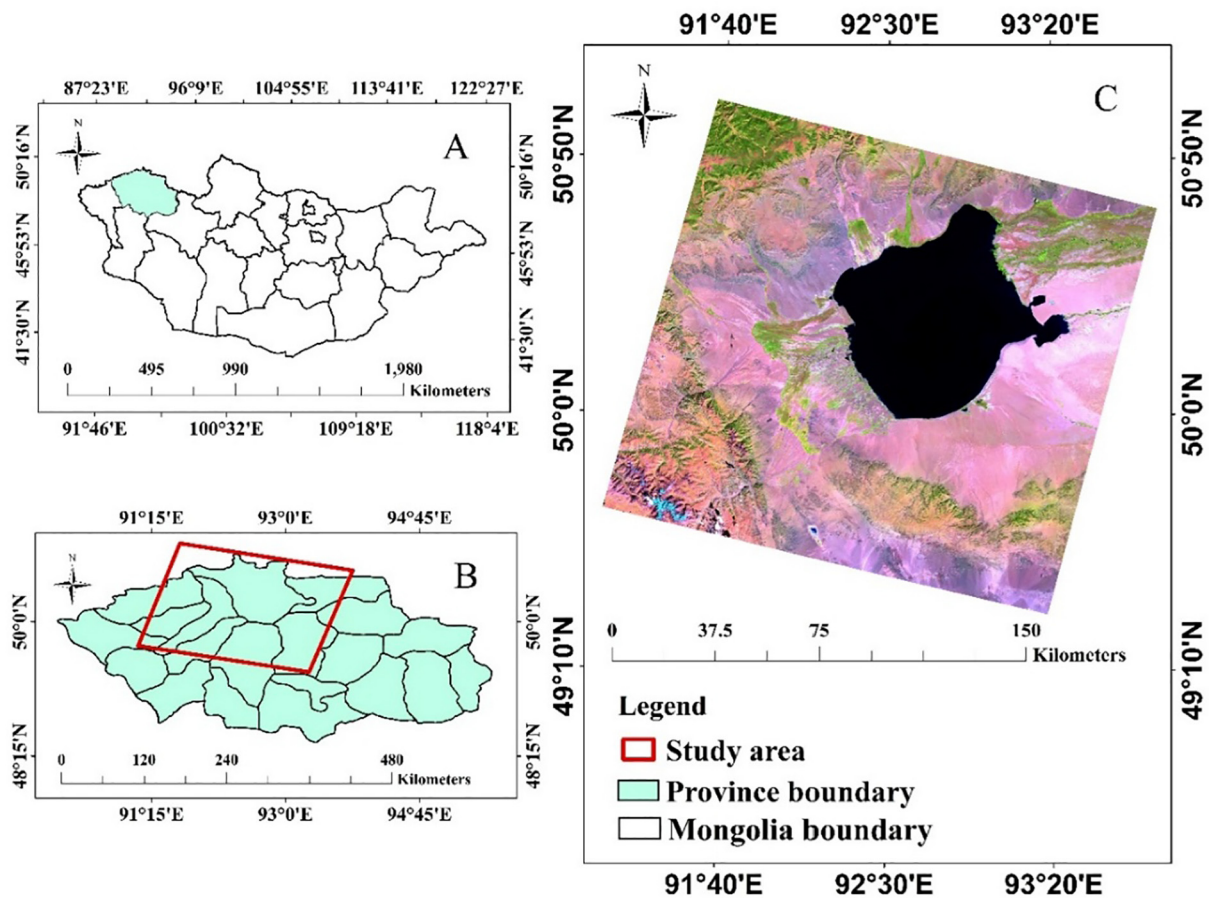


Fig. 1 – A geolocation map of the Mongolia (A) and the study site in theUvs Province (B), and a pseudo-colored picture in a combination of bands 5-4-3 for theUvs Lake Basin (C).

September. Temperatures reach -35°C or lower in the winter and 24°C or more in the summer. In general, the first autumn snowfall occurs in the first half of October and the last spring snowfall occurs in the middle of the second ten days of April and melts immediately. Winter snow cover lasts for 110–150 days a year. Annual precipitation falls between May and August of which 50% falls in July, 9% in September, 6% in May and the remaining 20% in the winter as snow. The annual precipitation is low around 150–200 mm [5].

2.2. Data

The Landsat images provide a wide spectral information at a scale of 60 km area which is suitable for studying land cover changes over a huge area [32]. As shown in Table 1, a series of Landsat images obtained during the summer seasons from 1995 to 2015 via TM, ETM+, and OLI sensors were collected from the website “<http://landsat.usgs.gov>”. Because the images were taken during the vegetative growing season,

Table 1 – The selected Landsat images and date of registration.

| Satellite | Sensor | Date of registration | Path/row | Resolution (m) |
|-----------|-------------------------|----------------------|----------|----------------|
| Landsat 5 | TM | 18/09/1995 | 141/025 | 30 |
| Landsat 5 | TM | 18/06/1998 | 141/025 | 30 |
| Landsat 5 | TM | 23/08/2001 | 141/025 | 30 |
| Landsat 7 | ETM+ (SLC-off) | 29/08/2004 | 141/025 | 30 |
| Landsat 7 | ETM+ (SLC-off) | 21/07/2007 | 141/025 | 30 |
| Landsat 5 | TM | 05/07/2010 | 141/025 | 30 |
| Landsat 8 | Operational Land Imager | 02/09/2013 | 141/025 | 30 |
| Landsat 8 | Operational Land Imager | 20/08/2015 | 141/025 | 30 |

the data should be appropriate for differentiating the spectral heterogeneity of land covers and therefore allow retrieval of valuable land cover information for change analysis. In Table 1, the SLC-off indicates the Landsat 7 ETM+ images were collected after May 31, 2003 when the Scan Line Corrector failed. The USGS provided two methods, i.e., phase one and phase two to fill the gaps of the SLC-off scene. The phase two method (<https://landsat.usgs.gov/filling-gaps-use-scientific-analysis>) incorporated more than two SLC-off scenes together to create a final product to fix the gap problem in the data. In addition to the images, the auxiliary datasets include maps of vegetation class, soil, forest, land use of this region and Google earth. These data provide support in determining the spatial distribution of land cover according to their natural characteristics.

2.3. Image processing and classification

The flowchart (Fig. 2) was followed, which describes the image processing and analysis for exploring the changes of land covers of this study. The FLAASH model was firstly applied to correct images for atmospheric water vapor, oxygen-carbon dioxide, and aerosol scattering for each image [33,34]. Then the Function-of-mask (Fmask) algorithm [35–37] was applied to fix the problem of clouds. The Fmask was first introduced by Zhu and Woodcock [36] for the use of Landsats 4–7 images and expanded by Zhu et al. [35] for Landsat 8 and Sentinel-2 images. Based on the cloud physical properties, the Fmask algorithm uses temperature, spectral variability, and brightness derived from the visible and SWIR bands to determine cloud probability of pixels for Landsats 4–7. After the cloud layer generation, a cloud shadow layer is produced using NIR and SWIR bands by applying the flood-fill transformation and a similarity measure of neighboring cloud heights. In contrast, the cirrus band is used to derive cloud based on a thresholding method for Landsat 8 instead of the method for Landsats 4–7.

Land cover classification was carried out using the support vector machine (SVM) and Maximum Likelihood Classifier (MLC). MLC tends to be easily influenced by the number of training samples in the derivation of land cover signatures. In general, the pixels should at least satisfy 10 times of the bands for each class in order to avoid the Hughes

phenomenon. For a classification using statistical classifier with a limited number of training samples, the accuracy may decrease as the number of bands used for classification increase due to the fail to maintain minimum statistical confidence and functionality in remotely sensed data [38]. It is particularly difficult in this situation to collect sufficient number of pure training samples from moderate resolution satellite images. In contrast, the SVM classifier needs only a few key samples for signature training. The SVM classification is therefore appropriate for dealing with the problems of image classification with large input dimensionality as well as the difficulties in collecting sufficient number of pure training pixels from images with a spatial resolution of 30 m or worse.

The SVM classification of land cover in this study is a machine learning based nonlinear discrimination for binary classification. The support vectors derived from the training samples of any two of the land cover types were used to formulate an optimal hyperplane or decision surface to distinguish the class of a candidate pixels belongings. For k types of land cover classification, a number of $k(k-1)/2$ decision surfaces are derived. Any image pixel is labelled as it locates exactly on a particularly optimal hyperplane. In other words, the multiclass SVM classification will not label a pixel to a class when the pixel falls beyond any other optimal margins.

For a supervised binary classification problem, if the training data are represented by $\{x_i, y_i\}$, $i = 1, 2, \dots, N$, and $y_i \in \{-1, 1\}$, where N is the number of training samples, $y_i = +1$ for class ω_1 and $y_i = -1$ for ω_2 . Let λ_i be the Lagrange multipliers, y_i be the labels of classes, x_i be the support vectors that correspond to non-zero Lagrange multipliers and x is the input vector (candidate pixel) that need to determine its class label, then the hyperplane can be fitted using the formula shown in Eq. (1),

$$f(x) = \sum_{i=1}^N \lambda_i y_i K(x_i, x) + w_0 \quad (1)$$

where $\sum_{i=1}^N \lambda_i y_i = 0$, $\lambda_i \geq 0$, $i = 1, 2, \dots, N$, and $K(x_i, x)$ is the kernel function which gives the weights of nearby data points in estimating target classes, and w_0 is the bias or error of the hyperplane fitting. The radial basis function shown in Eq. (2) was applied in this study. Following the research of land use land cover in [1], the gamma and penalty parameters of the RBF kernel was set to be 0.01 and 100 respectively.

$$K(x_i, x) = \exp(-\gamma \|x_i - x\|^2), \gamma > 0 \quad (2)$$

Following the IGBP classification scheme [20], the land cover is divided into forest (conifer and broadleaf), grassland, bareland, bare rock land, waterbody, sand, and glacier. The descriptions of the land cover types are given in Table 2. With the supplementary data such as topographic maps and provincial maps, the land covers were distinguished based on visual interpretation of satellite imagery using false color composition of the bands NIR, Red, and Green. Training samples of each feature class were collected and used to derive signatures of land cover types. In additional, new samples were also identified and collected via visual interpretation of the very high resolution images on Google Earth for the use of accuracy assessment. Both accuracy indices overall accuracy (OA) and kappa coefficient were calculated to assess

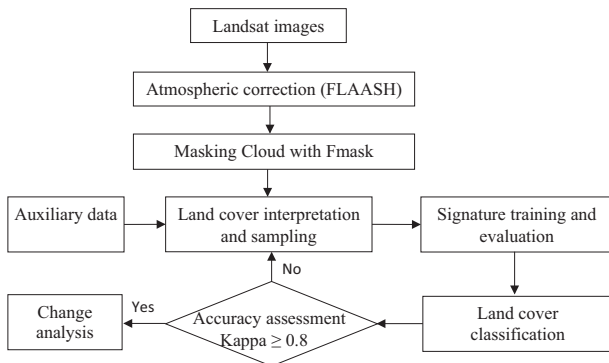


Fig. 2 – The flowchart for extracting land covers and change information from imagery.

Table 2 – Description of land cover types (the definition in IGBP classification scheme).

| Land classes | Description |
|------------------|--|
| Conifer forest | Lands dominated by evergreen woody vegetation with a percent cover >60% height exceeding 2 m |
| Broadleaf forest | Land dominated by wood with a percent cover >60% and height exceeding 2 m. Consists of broadleaf tree communities with an annual cycle of leaf-on and leaf-off periods |
| Grassland | The vegetation is dominated by grass species and less than 10% woody vegetation cover |
| Bareland | Land with exposed soil, build-up, roads and never has more than 10% vegetated cover over during any time of the year |
| Bare rock land | Lands dominated by bare rocks throughout the year |
| Waterbody | Rivers, lakes, streams and land with water |
| Sand | Land of spread sand that never has more than 10% vegetation covers during any time of the year |
| Glacier | Land of snow and ice |

the performance of the classification. In the results, the OA is presented in percentage (%) while kappa coefficient is ranged from 0 to 1.

Change analysis can be carried out based on the perspectives of brightness values (digital number/radiance/reflection) and thematic values (labelled/classified numbers) at the level of image pixels. As the change is implemented in a way of difference, ratio, and even change vector, the physical meaning of changes is not revealed. In other words, the method can only provide the information whether the pixel value is changed or not. While a qualitative method of change analysis is where classified values are being processed and therefore is able to provide the exact meaning of a change in each of the image pixels [1]. The method known as post-classification change detection [34] was applied for this purpose and consequently a form of “from-to” matrix was generated for each pair of two dates images.

3. Result

3.1. A view on the accuracy of multi-temporal land cover classifications

In Mongolia, land cover changes were mostly derived by maximum likelihood classifier (MLC). Therefore, the land cover classification was carried out by SVM and MLC classifiers in order to provide a comparison of the results for the society. As shown in Fig. 3, the SVM achieved an accuracy of OA between 87% and 95% and kappa between 0.83 and 0.92 for the images from 1995 to 2015, while the MLC achieved a lower

accuracy in both OA and kappa for all the images. In summary, the OA and kappa accuracy was averaged $92 \pm 2.45\%$ and 0.89 ± 0.03 for the SVM method and $87 \pm 2.01\%$ and 0.83 ± 0.03 respectively. The accuracy measures showed variation among the multi-temporal images and the classification methods. Although the SVM and MLC classifiers achieved almost identical accuracy with OA = 88% and kappa = 0.84 for the 1995 image, while the SVM appeared to be able to achieve an average kappa value of 0.06 larger than the MLC. The difference of classification performance between SVM and MLC is quite similar to the results published in articles [1,27]. Looking at the maps of SVM and MLC in Fig. 4, the MLC tends to exhibit a higher confusion in the vegetation classes, such as forest and grassland as well as the non-vegetative classes such as bare soil and bare rock. Consequently, the SVM classified land cover maps were used to derive change information of the Uvs Lake Basin.

3.2. The temporal trend of land cover changes

As shown in Fig. 5, the land covers maps in each of the serial multi-temporal images revealed a very high similarity of spatial distribution indicating reasonable classifications achieved that should be able to reflect the changes of land cover over the two decades appropriately. In 1995, the area of each land cover was 1888.48, 5086.08, 14244.14, 140.99, 65.2, 79.53, and 3727.06 km² for forest, grassland, bare land, bare rock, sand, glacier (snow), and water body respectively. The dominant types of land cover in this area was bare land, grassland, and then forest. Comparing to the area of each type of land

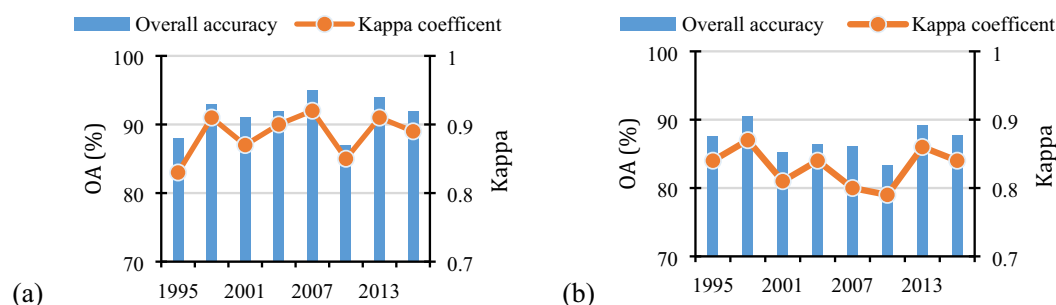


Fig. 3 – The kappa coefficient and overall accuracy of the classification using (a) SVM and (b) MLC methods.

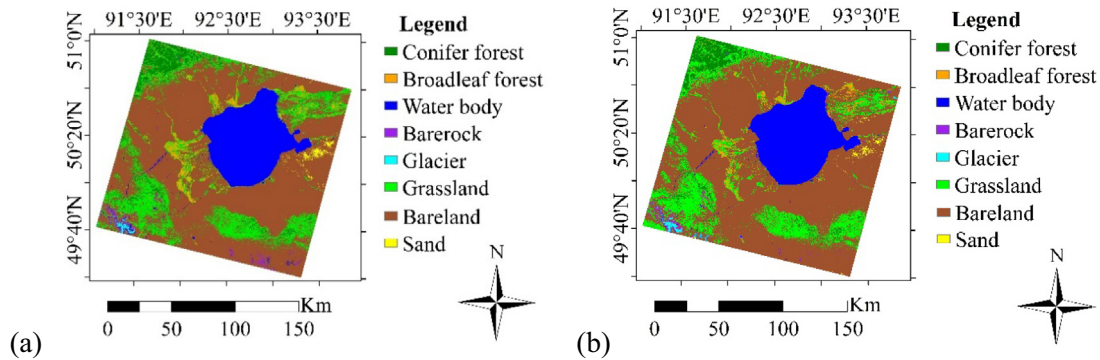


Fig. 4 – The land cover map of the Uvs Lake Basin in 1998 derived by the classifiers (a) SVM and (b) MLC.

cover in 1995, the temporal changes of the land cover areas during the 20-years period can be classified into three categories: insignificant change, increasing change, and decreasing change. Representative land cover types of each category was the waterbody for no change, the sands and bare land for increasing change, and the forest and glacier for decreasing change.

The area of water body increased by 1.7% in the early stage from 1995 to 2001 then decreased by 0.7% in the later stage from 2001 to 2015. On average, the water body areas changed $-0.7 \pm 1.5\%$ during the two decades. As it can be seen in Fig. 6, the curve of areal change rate of water body showed a tiny fluctuation in the two decades and therefore it could be concluded that the amount of water reserved in the Uvs Lake Basin was not changed. However, the coverage of glacier showed a considerable changes from 79.53 km² in 1995 to 29.97 km² in 2015. The curve of areal change rate of the glacier almost constantly declined during the period with a decreasing rate ranged between 18.2% and 62.3%. Change rate of the glacier areas was averaged $-44.5 \pm 13.2\%$.

Similarly, the coverage area of the forest type decreased from 1888.48 km² in 1995 to 1431.30 km² in 2015 and the decreasing rate was between 2.3% and 18.9% and averaged $-11.3 \pm 5.2\%$. The significant decreasing trend indicates natural disturbance such as forest fire and pest damage and/or anthropogenic disturbance such as logging and grazing occurred frequently and the decrease is most likely to lead to a series of land cover changes over time. In contrast, the sands and the bare soil showed dramatically increasing rates which ranged between 122.8% and 388.2% for the earlier and 228.5 and 335.7% for the later. As the constant increasing trend observed from the cumulated areal percentage in Fig. 6, the land over the Uvs Lake Basin was indeed continuously degraded during the two decades. The grassland coverage may be increased somewhat due to deforestation as well as recruitment over the bare land, however it may be decreased due to soil degradation. Although a variation of change rate was observed in the grassland, it eventually decreased by a small amount of area during the period from 1995 to 2015. In respect to the decreasing trend of the forest type, the expansion of the sand coverage is most likely to be increasing in the future. To summarize the changes of each land cover type, the data in areas and percentages were

shown in Table 3, in which the years 1995/2004/2015 present the start/middle/end points or the first and second decades of the 20-years period.

3.3. The change path delivered by the change matrices of land cover

A change matrix of the land cover types can provide details of the areal changes among the spans over the two decades. Based on pixel-by-pixel comparisons, the number of areas in each type of land cover was listed in a square matrix in which the value in each entry represents the from-and-to information of land cover types. The value in each of the diagonal entries means no change during the particular two years. Tables 4 and 5 show an example of the land cover change from 2013 to 2015 in the unit of km² and dimensionless percentage (%) respectively. As it can be seen, the forest (conifer and broadleaf) was mainly changed to grassland. There were 118.80 km² or 10.9% of the conifer changed and most of them (88.36 km² or 8.1%) were changed to grassland. Additionally, 170.22 km² out of the changed area of broadleaf forest (175.75 km²) had been transferred to grassland. In other words, 28.9% out of the 29.8% changed broadleaf forest was replaced by grassland. 97.2% of the bare land was retained while among the change areas there was 332.02 km² (2.2%) and 52.33 km² (0.4%) changed to grassland and sand tunes respectively. This indicates that the change path of bare land can be decomposition to form sand tunes or revegetation to grassland according to the changes occurring in soil moisture. In summary, the dynamics of land cover changes generally appeared to follow one of two paths, one the sequences from forest through grassland to bare land and finally sand dunes and the other is from glacier through bare land to sand dunes.

3.4. Spatial distribution of deforestation from 1995 to 2015

To summarize the overall changes of the deforestation in the area of Uvs Lake Basin during the two decades, the classified maps of land cover in 1995 and 2015 were recoded to generate binary forest and non-forest maps (Fig. 7a and b). These two thematic maps were then used to produce a change map to

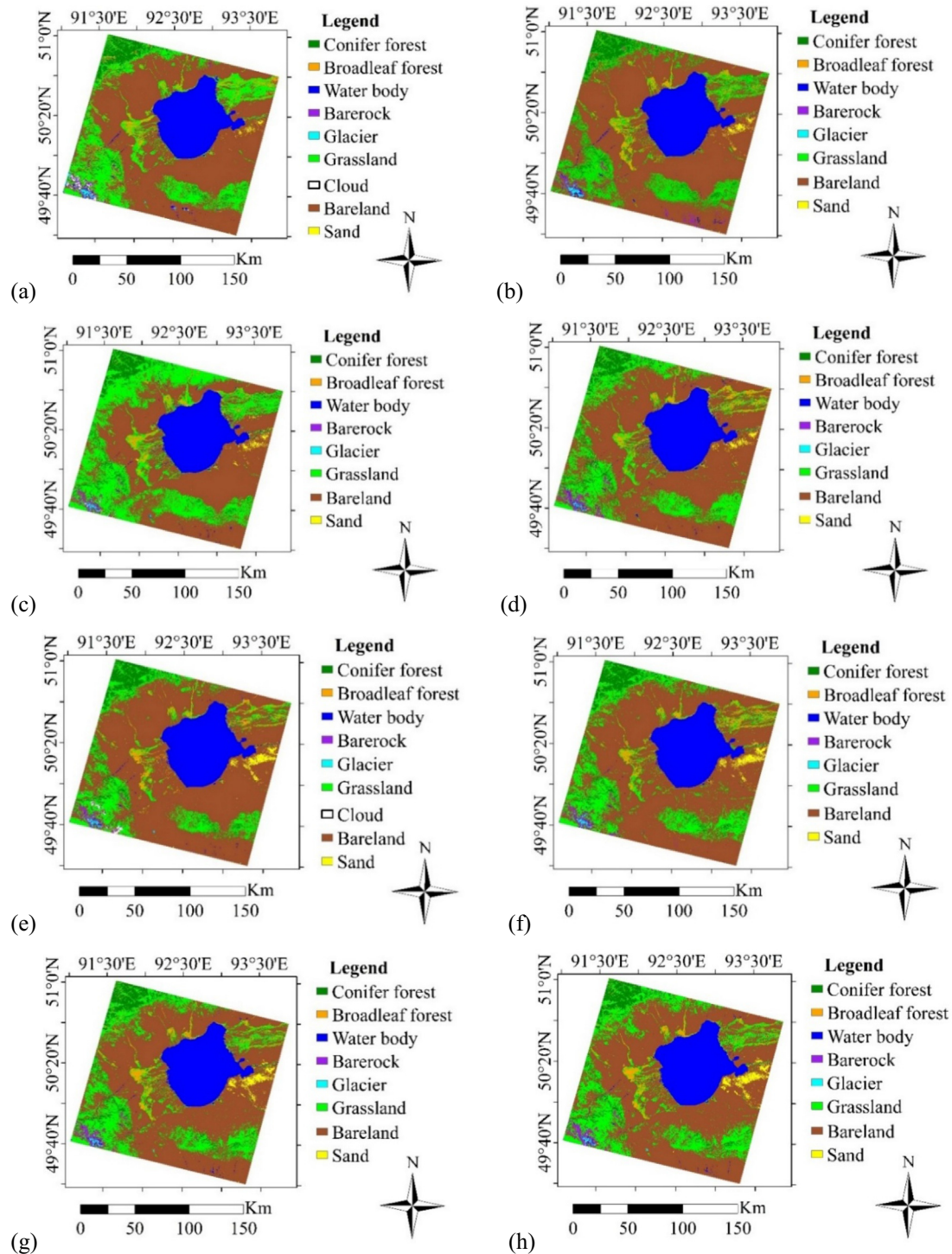


Fig. 5 – Land cover maps of the Uvs Lake Basin for the years (a) 1995, (b) 1998, (c) 2001, (d) 2004, (e) 2007, (f) 2010, (g) 2013, and (h) 2015.

highlight the locations of deforestation and forestation. Fig. 7c shows details of the spatial distribution of those losses and gains of the forest land. It can be seen that the deforestation mainly occurred in the north-east part of the Uvs lake and the reforestation mostly occurred in the south-west part of the lake and partially on the locations near the deforestation. Consulting with researchers at the National Agency for

Meteorology and Environmental Monitoring and the Uvs Lake Basin Projected Area Administration Office of Uvs Province in Mongolia, it is noted that some of the observed natural disturbances such as forest fire and insect damage as well as the anthropogenic disturbance such as logging was mainly located around the south-west and south-east parts of the lake (Fig. 7d).

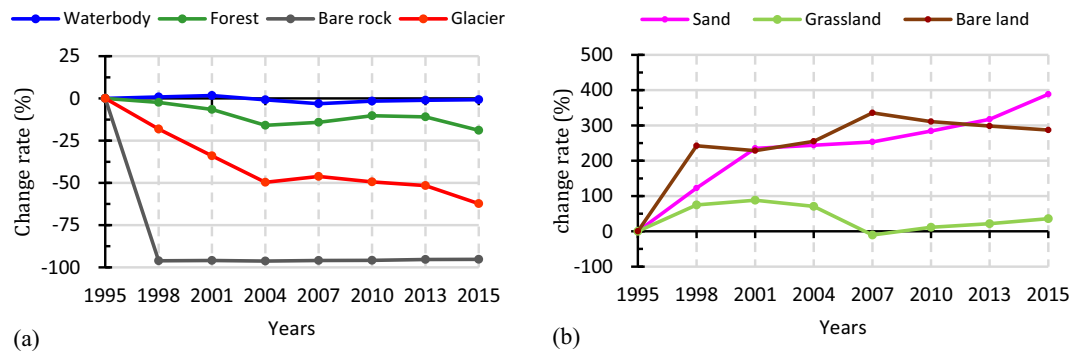


Fig. 6 – The trend of areal changes for the land cover in the Uvs Lake Basin. A negative or positive change rate indicates a decrease (a) or increase (b) situation respectively.

Table 3 – Statistical result of land cover change detection in two last decades.

| Land cover classes | 1995 | | 2004 | | 2015 | |
|--------------------|-------------------------|----------|-------------------------|----------|-------------------------|----------|
| | Area (km ²) | Area (%) | Area (km ²) | Area (%) | Area (km ²) | Area (%) |
| Conifer forest | 1338.29 | 5.30 | 1124.44 | 4.46 | 981.77 | 3.89 |
| Broadleaf forest | 550.18 | 2.18 | 462.67 | 1.83 | 449.53 | 1.78 |
| Grassland | 5086.08 | 20.16 | 6339.45 | 25.13 | 5060.58 | 20.06 |
| Bare land | 14244.14 | 56.45 | 13233.91 | 52.45 | 14515.2 | 57.53 |
| Bare rock | 140.99 | 0.56 | 109.60 | 0.43 | 176.38 | 0.70 |
| Sands | 65.20 | 0.26 | 224.34 | 0.89 | 318.33 | 1.26 |
| Glacier | 79.53 | 0.32 | 40.04 | 0.16 | 29.97 | 0.12 |
| Water body | 3727.06 | 14.77 | 3697.02 | 14.65 | 3699.71 | 14.66 |
| Total | 25231.47 | 100 | 25231.47 | 100 | 25231.47 | 100 |

Table 4 – Areal change matrix of the land cover types (km²) from 2013 to 2015.

| | | To 2015 | | | | | | | | |
|-----------|------------|---------|-----------|---------|-----------|--------|-----------|-----------|---------|------------|
| | | Conifer | Broadleaf | Water | Bare land | Sand | Bare rock | Grassland | Glacier | 2013 Total |
| From 2013 | Conifer | 974.46 | 2.53 | 0.06 | 27.73 | 0 | 0.19 | 88.36 | 0 | 1093.33 |
| | Broadleaf | 3.86 | 413.22 | 0.01 | 1.66 | 0 | 0 | 170.22 | 0 | 588.97 |
| | Water | 0.04 | 0 | 3677.3 | 5.96 | 0.02 | 2.71 | 0 | 0 | 3686.03 |
| | Bare land | 2.04 | 2.62 | 13.55 | 14441.92 | 52.33 | 4.85 | 332.02 | 0 | 14849.33 |
| | Sand | 0 | 0 | 0.49 | 5.41 | 265.71 | 0 | 0.01 | 0.49 | 272.11 |
| | Bare rock | 1.37 | 0 | 0.04 | 2.6 | 0.01 | 168.42 | 0.02 | 0 | 172.46 |
| | Grassland | 0 | 31.17 | 0 | 29.27 | 0 | 0.14 | 4470.18 | 0 | 4530.76 |
| | Glacier | 0 | 0 | 8.26 | 0.64 | 0.28 | 0 | 0 | 29.3 | 38.48 |
| | 2015 Total | 981.77 | 449.54 | 3699.71 | 14515.19 | 318.35 | 176.31 | 5060.81 | 29.79 | 25231.47 |

Table 5 – Percentage change matrix of the land cover types (%) from 2013 to 2015.

| | | To 2015 | | | | | | | | |
|-----------|-----------|---------|-----------|-------|-----------|------|-----------|-----------|---------|------------|
| | | Conifer | Broadleaf | Water | Bare land | Sand | Bare rock | Grassland | Glacier | 2013 Total |
| From 2013 | Conifer | 89.1 | 0.2 | 0.0 | 2.5 | 0.0 | 0.0 | 8.1 | 0.0 | 100 |
| | Broadleaf | 0.7 | 70.2 | 0.0 | 0.3 | 0.0 | 0.0 | 28.9 | 0.0 | 100 |
| | Water | 0.0 | 0.0 | 99.8 | 0.2 | 0.0 | 0.1 | 0.0 | 0.0 | 100 |
| | Bare land | 0.0 | 0.0 | 0.1 | 97.3 | 0.4 | 0.0 | 2.2 | 0.0 | 100 |
| | Sand | 0.0 | 0.0 | 0.2 | 2.0 | 97.6 | 0.0 | 0.0 | 0.2 | 100 |
| | Bare rock | 0.8 | 0.0 | 0.0 | 1.5 | 0.0 | 97.7 | 0.0 | 0.0 | 100 |
| | Grassland | 0.0 | 0.7 | 0.0 | 0.6 | 0.0 | 0.0 | 98.7 | 0.0 | 100 |
| | Glacier | 0.0 | 0.0 | 21.5 | 1.7 | 0.7 | 0.0 | 0.0 | 76.1 | 100 |

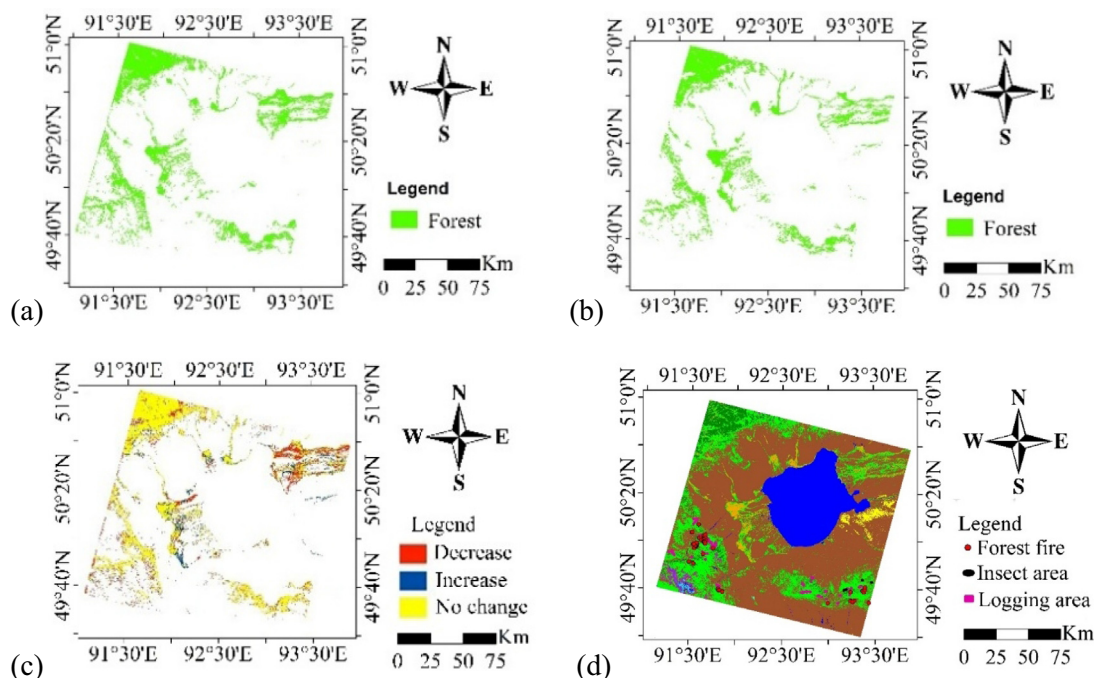


Fig. 7 – Thematic maps of the forest land over theUvs Lake Basin. Fig. 7(a) and (b) show the binary maps of the forest land in 1995 (a) and 2015 (b). Fig. 7(c) highlights the locations of the gained and lost forest and Fig. 7(d) displays the locations of those observed disturbances of forest fire, insect damage, and logging.

Forest degradation is generally a result of global warming and human activities caused by the economic value of trees and land grazing for livestock. The dominant tree species of the forest in theUvs Lake Basin ecoregion was Siberian larch (*Larix sibirica*). Larch timber is a popular material for external cladding as well as joinery, decking, and flooring. However the larch grows and regenerates quite slowly due to a short growing season in the cold continental climate. According to the meteorological data, the annual average temperature of the area ofUvs Lake Basin has increased by 2.26 °C over the last 70 years. In particular, the average temperature in the summer season has increased by 4 °C. In addition to the decreased precipitation over the last 25 years, the probability of forest fire and insect damage has therefore increased. As mentioned earlier, the majority of the deforested areas were on the north-east side of the lake. In contrast to the disturbance data observed and provided by the administrative agencies (Fig. 7d), where the deforestation implies a significant degradation over the latest 20 years and was probably due to illegal logging, grazing [39], and salinization [40].

4. Discussion

From the viewpoint of land-cover change analysis, a classification with 70–75% [38] or 80% overall accuracy [1,41] should be appropriate for deriving reliable change information. As noticed in Section 3.1, the accuracy of the land cover classification carried out by both SVM and MLC methods have shown some diversity for the multi-temporal Landsat images. On average, the SVM classification was able to achieve an accuracy at $OA = 92 \pm 2.45\%$ and $\kappa = 0.89 \pm 0.03$ which is better than

the MLC with $OA = 87 \pm 2.01\%$ and $\kappa = 0.83 \pm 0.03$. Because the SVM derived land cover maps with a performance better than the MLC and is substantially able to satisfy the requirement of accuracy for land cover mapping, it is recommended that the Mongolian society should consider using the SVM for regular land cover mapping of the semi-arid ecosystem.

TheUvs Lake Basin is located in the western Khangai of the southern Baikal region in Mongolia where the forest-steppe taiga occupies around only 6.5–7.6% of the region and is mainly distributed along the high mountain belt and accordingly the wooded area is small. In the previous section, the changes of land cover in the study site were derived almost every three years. As shown in Fig. 6, the curve of change rate of the forest land declined from 1995 to 2004, then elevated until 2010 and 2013, and again it decreased after that. The trend of forest land development is similar to previous investigations. According to Ykhanbai [42], forest degradation in Mongolia has increased from 1976 to 2006 which was mainly due to the expansion of forest fire and insect population as well as legal/illegal harvesting [43,44]. An inventory of natural forest conducted by theUvs Province government in 2011 showed that the forest area was significantly increased in theUvs Province. Compared to the inventory in 2007, the increment of forest land mainly occurred in some parts of the ecoregion such as the shrub lands of small groves and the broadleaf areas along river sides. Although the conifer forest in the Basin ecoregion decreased in 2011 the area of broadleaf forest expanded around 1300 ha and 1133 ha of the increment was increased mainly by willow (*Salix* spp.) [45]. The similarities between our results and the inventory studies indicates that the classified maps retrieved by this

study should be able to reflect the real situation of the development of forest land in the Basin ecoregion. Logging activities in the Basin ecoregion had a greater adverse effect on vegetation and soil properties than fire [43] and additionally most of the fires on the steppe and forest were caused by human activities [44]. Because forest ecosystem help to regulate climate amelioration, soil erosion, and provide habitat for flora, fauna, and microorganism, it is recommended that more effort should be put into the protection of the Basin ecoregion to achieve not merely the forest protection but also the ecosystem conservation.

The vegetation condition of a country is sensitive to change caused by the climate and human impact. The increasing use of natural resources also constantly affects the condition of pastureland as well as the Uvs Lake Basin ecoregion of the country [46]. The Basin ecoregion is mostly covered by bare land and grassland. Grassland is the main resource for animal husbandry. According to the statistics report of Uvs Province, grazing pressure in the Uvs Province has been increasing due to the significant increase of livestock population as the population in 2006 was 2x more than in 2000. Livestock is most also likely to cause unfavorable influences to the environment. The increasing population of livestock can directly impact on the reduction of grassland areas and thus convert it to bare land when accompanied with serious water stress such as the extreme drought that occurred in 2007 [47].

As mentioned earlier, the area of sands has almost increased by 5 times over the Basin ecoregion during the latest two decades. Because the significant increase of the sands was primarily contributed to by the transition of bare soil, it seems to be evidence of the process of land desertification in the Basin ecoregion. This kind of bare land transition is very close to the research of Batjargal [48]. The Buurug Sand located at the eastern part of the Uvs lake, recognized as the biggest sand dune of Mongolia, is where a constantly considerable sand movement was observed in the past. The eolian process suggests the most/medium/less amount of sand will be observed in the winter, the spring and autumn, and the summer with a rate of 40%, 22–28%, and 15% respectively [48]. Obviously, the eolian processes are constantly active and can cause significant soil moisture loss and erosion. An investigation reported in 1997 showed that wind erosion in Mongolia has caused soil losses of 35–50 tons/ha to cultivated land during the past 30 years [48], this is very similar to the increase of sand coverage found in this study. The dynamics of sand massifs indicate a process of land desertification. In addition, the climate change has affected the degree of evapotranspiration and dryness on the soil surface, which in turn may cause the rise of a dust storm [49]. Therefore, it is expected that the deflation of soil and even sand dunes movement in the Uvs Lake Basin will occur continuously.

The glacier in the Turgen Mountain accounts for more than 20% of the total coverage of the Mongolian glaciers [5]. The glacier increased slightly between 1940 and 1992 but decreased by 44.4% during the period from 1992 to 2011 [5,50,51]. The decrease in the latest two decades are similar to our results. Regional dynamics of permafrost is, under natural conditions, determined by climate change, especially by long-term changes in mean annual air temperature and precipitation [46]. Obviously, the significant decreasing rate of

glacier in the summertime is mainly the result of climate change or global warming [50]. According to the estimation of Dorjgotov et al. [5], air temperature of the Uvs Lake Basin will tend to rise by 4.0–4.4 °C for the upcoming 10–90 years and the precipitation will increase by 10–40% in the winter while most likely no significant changes will occur in the summer. This means that the climate will be hot, dry in the summer and warm with more snow in the winter in the Basin ecoregion. The latest research published in articles [52,53] highlighted the strength of RGB-UAV sensor in the detection of newly grown tree leaves which can provide valuable information for retrieving phenological events of trees and further growth of trees. In contrast to the moderate resolution remotely sensed data, satellite images with a decimeter level of spatial resolution are recommended for their capability of sensing tiny size targets for detecting crucial evidence of tree phenology, carbon stock [54], and the development of forest stand [55] as well as the changes caused by global warming.

5. Conclusion

This study investigated land cover changes in the Uvs Lake Basin ecoregion in western Mongolia during the period of 1995–2015 by remote sensing approaches. With the support vector Landsat multispectral signatures of forest (conifer and broadleaf), grassland, bare land, sand, bare rock, water, and glacier, the land cover maps were achieved with an average kappa value of 0.89 which was able to provide reliable information for deriving the change of land cover. The land coverage by each of the land cover types were in order, bare land, grassland, waterbody, forest, bare rock, glacier, and sand in 1995. Although the area of each land cover type changed during the investigation period, the coverage of the top four types remained in the same order. However, the three types with smaller areal percentage, i.e., bare rock, glacier, and sand were changed such that they were in the reverse order. The changes were mainly caused by the impact of natural and anthropogenic disturbances.

During the latest two decades, regarding the change of land cover of the study site the decrease of vegetation coverage including forest and grassland was around 482 km² which was around 1.91% of the study site. The process of greenness reduction was mainly caused by logging, grazing, and fires. In contrast, the increase of bare land and sand was 524 km² or 2.08% of the ecoregion. This was mainly contributed by soil degradation and eolian processes and even the interaction of natural processes (e.g. extreme drought and global warming) and human activities (such as reduction of greenness and over grazing). Due to global warming, the glacier had a decrease of around 50 km² or 0.10% coverage of the Basin ecoregion in the summer season. The reduction was small but it was 62% of the glacier area in 1995. The melted ice or snow flowed into the Uvs Lake and thus compensated for the water losses due to evaporation. As a result, the area of waterbody was reduced by only around 0.11% of the total area of the ecoregion. The reduction took only 0.73% part of the water coverage in 1995.

Details of the transition of land cover types can help to examine the situations of a land, especially for a protected ecoregion over time, in order to meet the need of appropriate

management for sustainability. As noted, the Uvs Lake Basin ecoregion has suffered from the impact of global warming, drought, wind erosion, and land degradation during the last two decades. In order to reduce the trend of soil degradation and forest development in the Basin ecoregion, more effort must be made to regulate the animal husbandry and logging activities as well as increase forest fire prevention. Instead of development activities, ecological tourism is likely to be able to provide economic contributions to the ecoregion and also provide economic support for natural landscape protection.

Conflicts of interest

The authors declare that there is no conflicts of interest.

Acknowledgements

The authors thank the National Agency for Meteorology and Environmental Monitoring and the Uvs Lake Basin Projected Area Administration Office of Uvs Province, Mongolia for their support in providing auxiliary data of the study site. Acknowledgement was also extended to Dr. Saulyegul Avlyush and Dr. Bathuu Nyam-Osor for providing valuable comments.

REFERENCES

- [1] Lin C, Wu CC, Tsogt K, Ouyang YC, Chang CI. Effects of atmospheric correction and pansharpening on LULC classification accuracy using WorldView-2 imagery. *Inform Process Agr* 2015;2:25–36.
- [2] Byambakhuu I, Sugita M, Matsushima D. Spectral unmixing model to assess land cover fractions in Mongolian steppe regions. *Remote Sens Environ* 2010;114:2361–72.
- [3] Rawat JS, Manish K. Monitoring land use/cover change using remote sensing and GIS techniques: A case study of Hawalbagh block, District Almora, Uttarakhand, India. *Egypt J Remote Sens Space Sci* 2015;18:77–84.
- [4] NRSC. Environment assessment technical reports: land cover assessment and monitoring in mongolia. National Remote Sensing Center, Mongolia. UNEP Environment Assessment Programme for Asia and the Pacific, Bangkok; 1998. p. 1–19.
- [5] Dorjgotov D, Jadambaa N, et al. Study compilation for the development of integrated water resource management plan of the Kharkhiraa and Turgen sub-river basin. Ulaanbaatar, Mongolia: Admon LLC; 2014. p. 1–221.
- [6] Pual M. Limnological aspects of the Uvs Nuur Basin in northwest Mongolia. Doctoral Dissertation, Technische Universität Dresden, Dresden, Germany. 2012.
- [7] Shiirevdamba T. Biological diversity in Mongolia. The first national report, Ulaanbaatar, Mongolia; 1998
- [8] Lin C, Popescu SC, Huang SC, Chang PT, Wen HL. A novel reflectance-based model for evaluating chlorophyll concentration of fresh and water-stressed leaves. *Biogeoscience* 2015;12:49–66.
- [9] Lin C, Dugarsuren N. Deriving the spatiotemporal NPP pattern in terrestrial ecosystems of Mongolia using MODIS imagery. *Photogramm Eng Remote Sens* 2015;81(7):587–98.
- [10] Popescu SC, Zhao K, Neuenschwander A, Lin C. Satellite lidar vs. small footprint airborne lidar: comparing the accuracy of aboveground biomass estimates and forest structure metrics at footprint level. *Remote Sens Environ* 2011;115(11):2786–97.
- [11] Lin C, Lin CH. Comparison of carbon sequestration potential in agricultural and afforestation farming systems. *Sci Agr* 2013;70(2):93–101.
- [12] Lin C, Thomson G, Lo CS, Yang MS. A multi-level morphological active contour algorithm for delineating tree crowns in mountainous forest. *Photogramm Eng Remote Sens* 2011;77(3):241–9.
- [13] Lo CS, Lin C. Growth-competition-based stem diameter and volume modeling for tree-level forest inventory using airborne LiDAR Data. *IEEE Trans Geosci Remote Sens* 2013;51(4):2216–26.
- [14] Lin C, Lo KL, Huang PL. A classification method of unmanned-aerial-systems-derived point cloud for generating a canopy height model of farm forest. In: *Proc IGARSS'16. Proceedings of geoscience and remote sensing symposium (IGARSS)*. IEEE International; 2016. p. 740–73.
- [15] Lin C, Trianingsih D. Identifying forest ecosystem regions for agricultural use and conservation. *Sci Agr* 2016;73(1):62–70.
- [16] Chen HM, Lin C, Chen SY, Wen CH, Chen CCC, Ouyang YC, et al. PPI-SVM-Iterative FLDA approach to unsupervised multispectral image classification. *IEEE J Sel Top Appl Earth Obs Remote Sens* 2013;6(4):1834–42.
- [17] Jovanovic D, Govedarica M, Sabo F, Bugarinovic Z, Novovic O, Beker T, et al. Land Cover change detection by using Remote Sensing: A case study of Zlatibor (Serbia). *Geographica Pannonica* 2015;19(4):162–73.
- [18] Yuan D, Elvidge CD, Lunetta RS. Survey of multispectral methods for land cover change analysis. *Remote Sensing Change Detection: Environmental Monitoring*. Michigan: Ann Arbor Press; 1998.
- [19] Tsolmon R, Genderen JV, Narantuya D. Database collection for land cover validation and monitoring on remote sensing/GIS in the west part of Mongolia. *Int Arch Photogramm, Remote Sens. Spatial Info Sci Beijing* 2008;B7:1343–6.
- [20] Dugarsuren N, Lin C, Tsogt, K. Land cover change detection in Mongolia in last decade using MODIS imagery. *The 32nd Asian Conf Remote Sens Taipei, Taiwan*; 2011.
- [21] Dugarsuren N, Lin C. Temporal variations in phenological events of forests, grasslands and desert steppe ecosystems in Mongolia: a remote sensing approach. *Ann For Res* 2016;59(2):175–90.
- [22] Batzorig E, Banzragch B. Mapping and monitoring principal crop land cover/use changes in Mongolia using remote sensing. In: *Proc IGARSS'12. proceedings of geoscience and remote sensing symposium (IGARSS)*. IEEE International; 2012. p. 2261–3.
- [23] Tsutsumida N, Saizen I, Matsuoka M, Ishii R. Land cover change detection in ulaanbaatar using the breaks for additive seasonal and trend method. *Land* 2013;2:534–49.
- [24] Pouteau R, Meyer J, Taputuarai R, Stoll B. Support vector machines to map rare and endangered native plants in Pacific islands forests. *Ecol Informatics* 2012;9:37–46.
- [25] Huang C, Davis LS. An assessment of support vector machines for land cover classification. *Remote Sens* 2002;23(4):725–49.
- [26] Koetz B, Morsdorf F, van der Linden S, Curt T, Allgöwer B. Multi-source land cover classification for forest fire management based on imaging spectrometry and LiDAR data. *For Ecol Manage* 2008;256:263–71.
- [27] Maryantica N, Lin C. Exploring changes of land use and mangrove distribution in the economic area of Sidoarjo District, East Java using multi-temporal Landsat images. *Inform Process Agr* 2017;4:321–32.
- [28] Petropoulos GP, Kontoes C, Keramitsoglou I. Burnt area delineation from a uni-temporal perspective based on Landsat TM imagery classification using Support Vector Machines. *Earth Obs Geoinf* 2011;13:70–80.

- [29] Deilmai RB, Ahmad BB, Zabihi H. Comparison of two classification methods (MLC and SVM) to extract land use and land cover in Johor Malaysia. *IOP Conf Series: Earth Environ Sci* 2014;20:1–7. <https://doi.org/10.1088/1755-1315/20/1/012052>.
- [30] Taati A, Sarmadian F, Mousavi A, Pour CTH, Shahir AHE. Land use classification using support vector machine and maximum likelihood algorithms by landsat 5 TM images. *Eng Phys Sci* 2015;12(8):681–7.
- [31] Srivastava PK, Han D, Rico-Ramirez MA, Bray M, Islam T. Selection of classification techniques for land use/land cover change investigation. *Adv Space Res* 2012;50:1250–65.
- [32] Duveiller G, Defourny P, Desclee B, Mayaux P. Deforestation in Central Africa: Estimates at regional, national and landscape levels by advanced processing of systematically-distributed Landsat extracts. *Remote Sens Environ* 2008;12:1969–81.
- [33] Jensen JR. *Introductory digital image processing: a remote sensing perspective*. 2nd, 3rd ed. USA: Englewood Cliffs, NJ: Prentice Hall; 2005.
- [34] ITT Visual Information Solutions. *Atmospheric correction module: QUAC and FLAASH User's Guide*. IDL; 2009.
- [35] Zhu Z, Wang Sh, Woodcock CE. Improvement and expansion of the Fmask algorithm: cloud, cloud shadow, and snow detection for Landsat 4–7, 8, and Sentinel 2 images. *Remote Sens Environ* 2015;159:269–77.
- [36] Zhu Z, Woodcock CE. Object-based cloud and cloud shadow detection in Landsat imagery. *Remote Sens Environ* 2012;118:83–94.
- [37] Frantz D, Röder A, Udelhoven Th, Schmidt M. Enhancing the detectability of clouds and their shadows in multitemporal dryland landsat imagery: extending fmask. *IEEE Geosci Remote S* 2015;12(6):1242–6.
- [38] Thenkabail PS, Gumma MK, Teluguntla P, Mehammed IA. Hyperspectral remote sensing of vegetation and agricultural crops. *Photogramm Eng Remote Sens* 2014;80:697–709.
- [39] WWF, Central Asia: Western Mongolia into southern Russia. <https://www.worldwildlife.org/ecoregions/pa1316> 2018. Retrieved May 6, 2018.
- [40] UNESCO,Uvs Nuur Basin, <http://whc.unesco.org/en/list/769>. Retrieved May 6, 2018.
- [41] Charles E. Olson, JR. IS 80% ACCURACY GOOD ENOUGH? The Future of Land Imaging (Operational) 2008; Pecora 17.
- [42] Ykhanbai H. Case studies on measuring and assessing forest degradation: forest resources degradation accounting in Mongolia. *Forest Resources Assessment Working Paper* 2009;176:1–9.
- [43] Park YD, Lee DK, Jamsran TS, Stanturf JA. Effects of forest fire and logging on forest degradation in Mongolia. In: Stanturf, John A., editor. *Proceedings of the 14th biennial southern silvicultural research conference*. Gen. Tech. Rep. SRS–121. Asheville, NC: U.S. Department of Agriculture, Forest Service, Southern Research Station; 2010. p. 571–5.
- [44] Erdenetuya M. Fire occurrence and burning biomass statistics in Mongolia. *The 33rd Asian Conference of Remote Sensing*. Thailand; 2012.
- [45] Ganbat U, et al. *Report of natural inventory study*. Ulaanbaatar, Mongolia: Grand forest LLC; 2011.
- [46] Adyasuren TS, Erdenetuya M. Vegetation cover monitoring in Mongolia plateau using remote sensing technology. *Environ Remote Sens Monit Mongolia* 2007:73–86.
- [47] Climate change studies in Mongolia: Potential impacts of climate change and vulnerability and adaptation assessment for grassland ecosystem and livestock sector in Mongolia 2003;1–9.
- [48] Batjargal Z. Desertification in Mongolia. *Proceedings of an inter. workshop on rangeland desertification*. Ulaanbaatar, Mongolia: RALA Report 1997;200:108–113.
- [49] Nyamtseren M, Jamsran TS, Sodov Kh, Magsar E. *Desertification atlas of Mongolia*; 2013. p. 135.
- [50] Tsutomu K, Gombo D. Recent glacier variations in Mongolia. In: *Proceeding of the 3rd International workshop on terrestrial change in Mongolia*, Tsukuba, Japan; 2004. p. 20–4.
- [51] Sharkhuu H. Recent changes in the permafrost of Mongolia. In: *Proceedings of the VII international permafrost conference*, Switzerland; 2003. p. 1029–34.
- [52] Lin C, Chen SY, Chen CC, Tai CH. Detecting newly grown tree leaves from unmanned-aerial-vehicle images using hyperspectral target detection techniques. *ISPRS J Photogramm Remote Sens* 2018;142:174–89.
- [53] Chen SY, Lin C, Tai CH, Chuang SJ. Adaptive window-based constrained energy minimization for detection of newly grown tree leaves. *Remote Sensing* 2018;10:96. <https://doi.org/10.3390/rs10010096>.
- [54] Lin C, Thomson G, Popescu SC. An IPCC-compliant technique for forest carbon stock assessment using airborne LiDAR-derived tree metrics and competition index. *Remote Sens* 2016;8:528. <https://doi.org/10.3390/rs8060528>.
- [55] Lin C, Tsogt K, Zandraabal T. A decompositional stand structure analysis for exploring stand dynamics of multiple attributes of a mixed-species forest. *For Ecol Manage* 2016;378:111–21.